A Wearable Device for Real-Time Motion Error Detection and Vibrotactile Instructional Cuing

Beom-Chan Lee, Shu Chen, and Kathleen H. Sienko, *Member, IEEE*

***Abstract*—We have developed a mobile instrument for motion instruction and correction (MIMIC) that enables an expert (i.e., physical therapist) to map his/her movements to a trainee (i.e., patient) in a hands-free fashion. MIMIC comprises an expert module (EM) and a trainee module (TM). Both the EM and TM are composed of six-degree-of-freedom inertial measurement units, microcontrollers, and batteries. The TM also has an array of actuators that provide the user with vibrotactile instructional cues. The expert wears the EM, and his/her relevant body position is computed by an algorithm based on an extended Kalman filter that provides asymptotic state estimation. The captured expert body motion information is transmitted wirelessly to the trainee, and based on the computed difference between the expert and trainee motion, directional instructions are displayed via vibrotactile stimulation to the skin. The trainee is instructed to move in the direction of the vibration sensation until the vibration is eliminated. Two proof-of-concept studies involving young, healthy subjects were conducted using a simplified version of the MIMIC system (pre-specified target trajectories representing ideal expert movements and only two actuators) during anterior–posterior trunk movements. The first study was designed to investigate the effects of changing the expert–trainee error thresholds (0.5°, 1.0°, and 1.5°) and varying the nature of the control signal (proportional, proportional plus derivative). Expert–subject cross-correlation values were maximized (0.99) and average position errors (0.33°) and time delays (0.2 s) were minimized when the controller used a 0.5° error threshold and proportional plus derivative feedback control signal. The second study used the best performing activation threshold and control signal determined from the first study to investigate subject performance when the motion task complexity and speed were varied. Subject performance decreased as motion speed and complexity increased.**

***Index Terms*—Balance control, instructional cues, intelligent tutoring systems, movement, rehabilitation, vibrotactile.**

I. Introduction

PHYSICAL rehabilitation has been shown to improve sensory integration, motor coordination, and strength in patient populations with balance or vestibular disorders, stroke, and traumatic brain injuries [1]–[4]. During conventional rehabilitation and training, physical therapists communicate proper execution of an exercise to patients through a combination of verbal instruction, demonstration, and/or physical guidance. Instruction and demonstration are provided prior to and/or during the execution of the rehabilitation exercise and are typically used in combination with extrinsic (or augmented) feedback [5]. The impact of feedback on motor learning varies as a function of the frequency, delay, and precision with which information is provided [6]. Physical guidance involves the manual manipulation of a patient's body or body segment(s) in order to facilitate the completion of a task that a patient may not otherwise be able to perform on his/her own [7]. While physical guidance improves the patient's ability to accurately replicate the desired trajectory or movement, it does so at the expense of providing a patient with the ability to detect and correct errors [7], a critical aspect of motor learning [8], [9].

Vibrotactile stimulation, typically generated by rotary or linear electromechanical actuation or pneumatic balloon actuation, has been used to provide haptic feedback via the skin. Furthermore, characteristics of the vibratory signals such as frequency, amplitude, waveform, and duration have been modulated to convey information [10]. Arrays of actuators have been used to display basic shapes [11], [12] and textual characters [13], [14]; provide directional cues for navigation [15]; maintain spatial orientation and situational awareness during flight [16]; complement visual and auditory cues for improved user perception in virtual, augmented, and real environments [17]; decrease postural sway during quiet and perturbed stance in both individuals with vestibular deficits and older adults [18]–[22]; and retrain knee joint loading during gait [23].

Technologies that augment traditional rehabilitation practices in the clinical setting or increase compliance in at-home based exercise programs have the potential to provide both instructions regarding the intended movements and real-time or delayed feedback. Lieberman and Breazeal developed a real-time wearable vibrotactile feedback suit to facilitate upper limb human motor learning [24]. Subjects were asked to replicate upper limb motion presented via prerecorded video while receiving vibrotactile feedback based on passive motion tracking measurements whenever an error between the target motion and the subject's motion occurred. The feedback control signal used in this study was solely based on errors of joint angles. Vibrotactile feedback contributed to a decrease in motion errors and an accelerated motor task-learning rate compared to prerecorded video-based instructional cues when the arm motion was produced using a hinge joint. Rotational joint motions were not improved with statistical significance. The authors noted that video or optical-based motion tracking

Manuscript received March 12, 2010; revised October 28, 2010; accepted February 24, 2011. Date of publication April 19, 2011; date of current version August 10, 2011. This work was supported by the National Science Foundation's CAREER program (RAPD-0846471, funded under the American Recovery and Reinvestment Act of 2009) and the University of Michigan Office of Technology Transfer.

B. C. Lee is with the Department of Mechanical Engineering, University of Michigan, Ann Arbor, MI 48109 USA (e-mail: channy@umich.edu).

S. Chen is with the Institute of Gerontology, University of Michigan, Ann Arbor, MI 48109 USA (e-mail: chenshu@med.umich.edu).

K. H. Sienko is with the Department of Mechanical Engineering and the Department of Biomedical Engineering, University of Michigan, Ann Arbor, MI 48109 USA (e-mail: sienko@umich.edu).

Color versions of one or more of the figures in this paper are available online at http://ieeexplore.ieee.org.

Digital Object Identifier 10.1109/TNSRE.2011.2140331

of the human body is not feasible for use outside of a laboratory environment due to the expense and size of the equipment.

Several other recent studies have developed and assessed kinesthetic motion guidance systems for upper limb motion guidance that use a control signal proportional to the position error between the target and subject [25]–[27]. Both the Sergi *et al.* (2008) and Kapur *et al.* (2010) kinesthetic guidance systems employ magnetic motion tracking technologies. Recent advances in micro-electro-mechanical system technology such as the miniaturization of inertial measurement units (IMUs) have provided a platform for real-time motion tracking in unconstrained environments [28]–[31]. Van der Linden *et al.* (2009) leveraged this portable and low-cost technology for their upper limb motion study focused on teaching violin bowing techniques.

The majority of kinesthetic-based motion guidance techniques explored to date have provided a control signal proportional to the position error between the target and the subject, which may or may not be varied in terms of magnitude or frequency based on the magnitude of the error. However, in light of the known time delay associated with perceiving, processing, and responding to vibrotactile cues (our pilot studies indicate < 250 ms), we hypothesize that performance might be further improved if the rate of change of position or other predictive information were used to generate the feedback control signal. In a recent study performed by Wall and Kentala [32], several control signals were used to activate vibrotactile trunk feedback during computerized dynamic posturography in a subject population with vestibular loss. Specifically, they evaluated the following control signals: proportional to the measured tilt angle (P), proportional to the rate of change of tilt angle (D), and a combination of the P and D signals (PD). Their findings demonstrated that all evaluated control signals reduced trunk tilt, but that the PD control signal produced significantly smaller trunk tilt values compared to either P or D feedback.

This paper describes the design, development, and initial assessment of a wearable, wireless, IMU-based expert–trainee motion error detection and vibrotactile instructional cuing technology called MIMIC (mobile instrument for motion instruction and correction). This technology enables an expert to map his/her movements to a trainee in hands-free fashion using IMUs, microcontrollers, and vibrating actuators. The goal of this technology is to provide vibrotactile instructional cues to a trainee based on the motion of an expert. In what follows, we 1) describe the MIMIC's hardware and software components, 2) quantitatively assess a simplified version of the MIMIC's effectiveness in a young healthy pilot subject population during simple trunk bend exercises, and 3) determine the best control signal and movement error threshold for slow trunk-based vibrotactile instructional cuing.

II. Methods

A. MIMIC Design Overview

An overall schematic representation of the MIMIC is given in Fig. 1. The wearable IMU-based expert–trainee motion error detection and vibrotactile instructional cuing device is composed of an expert module (EM) and trainee module (TM) that are utilized by a physical therapist and patient, respectively. Each module includes a six-degree-of-freedom IMU, microcontroller unit (MCU), Bluetooth module, data-saving module, and battery. The TM additionally has an array of tactors that provide vibrotactile stimulation to the skin. The expert's body motions are sensed by the EM IMU and processed by an extended Kalman filter (EKF) estimation algorithm embedded in the MCU. The estimated expert motion is transmitted wirelessly to the TM through Bluetooth communication, and based on the computed difference between the expert and trainee motion, directional instructions are displayed via vibrotactile stimulation to the skin. The trainee is instructed to move in the direction of the vibration until the stimulus ceases. All information related to the body motion of the expert and trainee and the tactor stimulation history are recorded in the data-saving module for postprocessing and analysis.

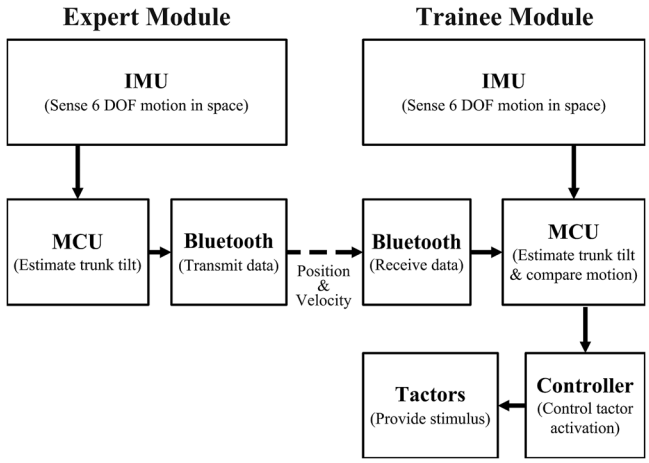

Fig. 1. System configuration.

B. Hardware

The hardware architecture is organized in layers to minimize size and enable easy access for replacement or maintenance. The main layer is equipped with an MCU, Bluetooth module, and data-saving module. Communication between the main layer and sensor layer is achieved with serial data communication through a wired connection.

The primary purposes of the MCU are to log IMU data, capture raw angular rates and linear accelerations, estimate body motion using an EKF, generate a control signal for vibrotactile stimulation, manage data communication, and store data in text format on a data-saving module. For embedded application systems, MCUs such as the ATMEL ATmega 128 provide acceptable computational performance with minimal power consumption and low cost.

The sensory layer comprises a tri-axial linear accelerometer (Freescale Semiconductor, Inc., MMA7260Q) and two gyroscopes (InvenSense, Inc., IDG-300). The accelerometers used in this prototype have a sensitivity range of ± 4 g with a bandwidth of 350 Hz along each axis. The gyroscopes have a range of $\pm 500^\circ/\mathrm{s}$. IMU data is sampled at 300 Hz.

Two coin-style eccentric mass pager motors (Samsung Electro-Mechanics, DMJBRK30O), shown in Fig. 2(c) and subsequently referred to as tactors, were selected to provide vibrotactile stimulation based on their small size and weight,

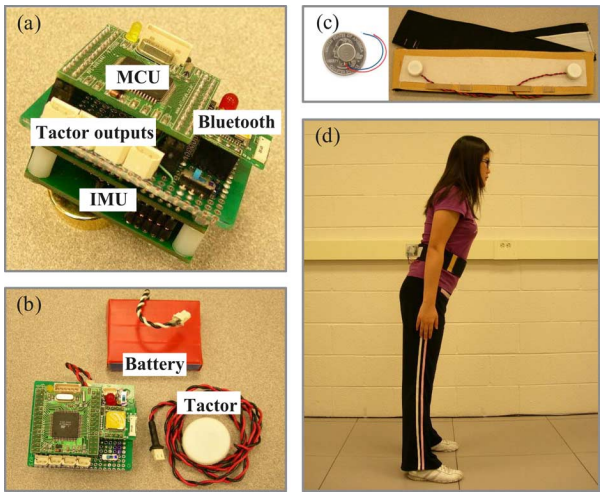

Fig. 2. Hardware architecture. (a) Hardware layers. (b) Hardware system components. (c) Coin-style pager motors and belt. (d) Trainee wearing MIMIC device.

low cost, and minimal power consumption. The spin-up time for the selected tactors to reach maximum rotational vibration is on the order of 90 ms. Each has an operating voltage range of 2.5–3.5 V at 65 mA, a frequency of 200 Hz at 3.0 V, a weight of 1.2 g, and a vibration quantity of 0.84 g root-mean-square.

Wireless communication of estimated expert motion data is provided by the Bluetooth module (Comfile Technology Inc., ACODE 330). This module supports Bluetooth 2.0 with SPP interface and also supports simultaneous operation of multiple devices, thereby enabling an expert to engage with more than one trainee. The Bluetooth protocol provides sufficient bandwidth to transmit data—approximately 0.23 Mb/s in symmetric mode.

The data-saving module allows the main processor to store numeric data such as raw or state space representation 3D motion data on an SD memory card for postprocessing. Each module is powered by a rechargeable lithium ion battery with a rating of 900 mAh.

C. Software

To maximize the embedded MCU performance, a component-based software architecture was designed to carefully manage computational resources, prioritizing real-time motion capture and estimation, data transmission, and data-saving capabilities. The core software architecture implemented in the MCU is the same in both the EM and TM. The only software difference between the two modules is the number of data packets communicated to/from peripheral interfaces; the TM acquires raw linear accelerations and angular velocities from the trainee IMU as well as estimated tilt data from the EM.

Tilt estimates were computed based on an Euler-angle-based EKF [33] with four state variables. Two of the state variables (roll and pitch angular positions) were calculated from the output of the tri-axial accelerometer [34]. The remaining two state variables (roll and pitch angular velocities) were acquired directly from the gyroscopes. The EKF, based on a first-order linear state transition model and nonlinear measurement model, estimated tilt at a rate of 100 Hz with accuracy better than 0.25° confirmed by tilt table testing. The implemented EKF continuously measures tri-axial accelerations in order to correct for drift error based on the assumption that human trunk acceleration is bounded and averages to zero over an extended period of time [35]. The real-time estimation algorithm can support both Euler angle and quaternion computations.

For the two control signals chosen for separate evaluation in this study, the difference in position between the expert and trainee was used to generate the error term for the proportional (P) control signal, while differences in both position and velocity between the expert and trainee were used to generate error terms for the proportional plus derivative (PD) control signal

$$\text{Error} = (\theta_{\text{expert}} - \theta_{\text{trainee}}) + K_d(\dot{\theta}_{\text{expert}} - \dot{\theta}_{\text{trainee}}) \quad (1)$$

where θ represents the estimated tilt angle in degrees and $\dot{\theta}$ represents the angular velocity of tilt in $^\circ/\text{ms}$. The angular velocity was calculated by subtracting sequential tilt angle estimates and dividing by the 10 ms estimation interval (corresponding to the 100 Hz tilt estimation rate). K_d is a constant chosen to be 0.5 ms based on a previous study [32], [36]. Because this control signal incorporated velocity as well as position error terms, it effectively reduced the tactor activation threshold, theoretically enabling the subjects to quicken their response. The use of a control signal based solely on velocity error was eliminated from consideration based on the results of a pilot study in which this signal produced excessive oscillatory trunk movements in subjects. If the absolute value of the error signal exceeded the specified expert–trainee error threshold, an "attractive" vibrotactile cue was provided to the trainee until the error signal dropped below the threshold value. Vibrotactile stimulation was not graded according to the magnitude of the error signal; tactor activation was binary in nature (either on or off).

D. Subjects

The first of two proof-of-concept studies using the MIMIC employed five young $(23.4 \pm 3.3$ years) healthy naïve subjects (three male, two female). The follow-up study employed eight young $(26.5 \pm 1.3$ years) healthy naïve subjects (five male, three female). The University of Michigan Institutional Review Boards approved the experimental protocol, which conformed to the Helsinki Declaration. Informed consent was obtained from each subject prior to the start of the experiment.

E. Experimental Protocol

The first study was designed to investigate the effects of changing the vibrotactile stimulation activation threshold and varying the nature of the control signal. The follow-up study used the best-performing activation threshold and control signal determined from the first study to investigate subject performance when the motion task complexity and speed were increased. Subjects participating in both studies were instrumented with the TM and instructed to 1) stand with their feet parallel approximately 15 cm apart (indicated by floor markings) and 2) "move in the direction of the vibration until the vibration stops." This latter instruction represents attractive cuing. Standard foam earplugs and earmuffs were provided to eliminate environmental and tactor noise. One tactor was placed

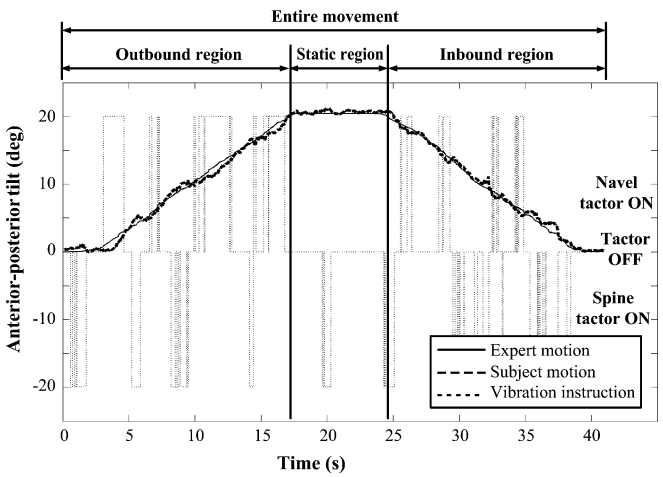

Fig. 3. Representative sample data when the expert–trainee activation threshold was set at 0.5° and a PD control signal was provided. Solid, dashed, and dotted lines represents the expert motion, subject motion, and vibration instruction, respectively. Positive values indicate movement in the anterior direction.

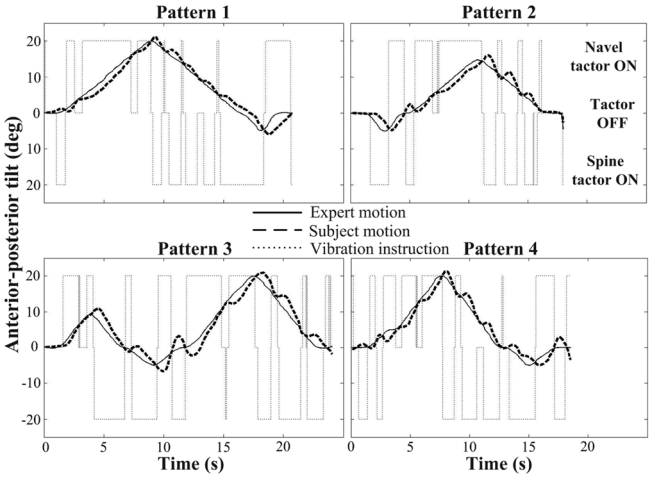

Fig. 4. Representative sample data in which the four different patterns were provided. Solid, dashed, and dotted lines represent the expert motion, subject motion, and vibration instruction, respectively. Positive and negative values indicate movement in the anterior and posterior directions, respectively.

near the navel and another near the spine at approximately the L4/L5 lumbar level. Prior to data collection, subjects were provided with acclimatizing tactor stimulation.

In the first study, subjects were asked to replicate a pre-specified anterior–posterior (A/P) trunk movement, subsequently referred to as "expert motion," by moving toward the vibrotactile instructional cues. The expert motion consisted of an anterior 20° trunk bend followed by a 6 s static hold at 20° and a posterior trunk bend to return to neutral upright stance (refer to solid line in Fig. 3). The anterior and posterior 20° trunk bends were performed at a rate of approximately $1.12°/\mathrm{s}$. Note that each subject was asked to bend only at the waist in response to the vibrotactile cues while they were performing the task.

Three expert–trainee error thresholds (0.5°, 1.0°, and 1.5°) and two control signals (P and PD) were evaluated in this study. Each subject performed three repetitions of the six possible control signal and error threshold combinations, totaling 18 trials. The presentation of trial type was randomized and no practice trials were provided. In addition, pre-/post-baseline data were collected to assess any potential training effects. All experimental trials were performed with eyes closed.

In the follow-up study, subjects were presented with the same pre-specified anterior–posterior (A/P) trunk movement used during the first study, but at three different speeds: slow (approximately $1.12°/\mathrm{s}$), medium (approximately $2.0°/\mathrm{s}$), and fast (approximately $4.0°/\mathrm{s}$). Subjects were also asked to use the vibrotactile cues to replicate four additional and more challenging A/P expert trunk motion patterns with variable speeds (Fig. 4). The follow-up study leveraged the results from the first study and therefore only the best performing control signal (PD) and error threshold (0.5°) were used. Each subject performed three repetitions for each speed of the simple motion and three repetitions of each of the four more challenging patterns, totaling 21 trials. The presentation order of both speed and pattern type were randomized. One practice trial for each speed and pattern was provided.

F. Data Analysis Methodologies

All postprocessing was performed using MATLAB (The MathWorks, Natick, MA). To characterize subjects' ability to replicate the expert motion, a cross-correlation analysis of the expert and subject trunk tilt angle was performed. The output of the cross-correlation analysis was 1) a cross-correlation value ranging between 0 and 1, with 1 indicating perfectly matched motion and 2) a time delay, with a positive delay indicating a time lag between the expert and trainee motion. Position error was defined as the average difference between the expert and subject position in degrees. For the purpose of data analysis, each trial from the first study was split into outbound, static, and inbound regions (shown in Fig. 3) corresponding to the anterior trunk bend, static hold at 20°, and posterior trunk bend to the neutral upright position, respectively. The composite movement was defined as the entire sequence of regions. The position error in the outbound and inbound regions characterizes performance during dynamic motion, while the position error in the static region characterizes performance during the static trunk bend.

Statistical analysis was performed using linear mixed effects models (LMM). One particularly desirable feature of this analytical methodology is that it takes into account the likely correlation of repeated measurements performed on the same subject. Dependent variables were cross-correlation value, time delay, and position error. The primary focus of the analysis was to estimate the effects of activation threshold and control signal on the dependent variables while accounting for the correlation of the observations' random intercepts associated with subjects and replicated measures. Hypotheses for the main effects of activation threshold and control signal and their interactions were tested using an F-test. Post-hoc analysis for each dependent variable was performed using Sidak's method. To assure the assumptions of the LMM (in particular normality and constant variance of residual variance for the time delay and position error), the dependent variable was expressed on a logarithmic scale.

TABLE I
STATISTICAL ANALYSIS RESULTS ($n = 5$) FOR ACTIVATION THRESHOLD (AT) AND CONTROL SIGNAL (CS). RESULTS FOR ALL DEPENDENT VARIABLES EXCEPT CROSS-CORRELATION ARE EXPRESSED ON A LOGARITHMIC SCALE. *IN THE PRESENCE OF SIGNIFICANT CONTROL SIGNAL BY ACTIVATION THRESHOLD INTERACTION, ESTIMATES OF MAIN EFFECTS ARE NOT INTERPRETABLE AND THEREFORE NOT REPORTED

Dependent variable	Effects	Estimate	DF	F Value	Pr>F
Cross correlation (Entire)	AT (1 vs 3)	0.0318	2,72	15.86	<0.0001
	AT (2 vs 3)	0.0129			
	CS (P vs PD)	-0.0287	1,72	38.29	<0.0001
Position error (Outbound)	AT (1 vs 3)	-0.5300	2,72	50.64	<0.0001
	AT (2 vs 3)	-0.2022			
	CS (P vs PD)	0.6627	1,72	233.1	<0.0001
Position error (Static)	AT (1 vs 3)	-0.4245	2,72	7.09	0.0016
	AT (2 vs 3)	-0.0983			
	CS (P vs PD)	0.6516	1,72	45.71	<0.0001
Position error (Inbound)	AT X CS		2,70	4.49	0.0147
Position error (Entire)	AT (1 vs 3)	-0.5571	2,72	95.09	<0.0001
	AT (2 vs 3)	-0.2423			
	CS (P vs PD)	0.6906	1,72	435.84	<0.0001
Time delay (Entire)	AT (1 vs 3)	-0.7599	2,72	3.40	0.0388
	AT (2 vs 3)	-0.2489			
	CS (P vs PD)	1.1466	1,72	22.34	<0.0001

TABLE II
STATISTICAL ANALYSIS RESULTS ($n = 8$) FOR SPEED (S) AND PATTERN (P). RESULTS FOR ALL DEPENDENT VARIABLES EXCEPT CROSS-CORRELATION ARE EXPRESSED ON A LOGARITHMIC SCALE

Dependent variable	Effects	Estimate	DF	F Value	Pr>F
Cross correlation (Entire)	S (1 vs 3)	0.0121	2,46	65.15	<0.0001
	S (2 vs 3)	0.0061			
	P (1 vs 4)	0.0207	3,69	20.53	<0.0001
	P (2 vs 4)	0.0001			
	P (3 vs 4)	-0.0088			
Position error (Entire)	S (1 vs 3)	-0.9461	2,46	141.56	<0.0001
	S (2 vs 3)	-0.3128			
	P (1 vs 4)	-0.2720	3,69	16.18	<0.0001
	P (2 vs 4)	-0.1521			
	P (3 vs 4)	-0.0854			
Time delay (Entire)	S (1 vs 3)	0.0539	2,46	3.12	0.0535
	S (2 vs 3)	0.1769			
	P (1 vs 4)	-0.1936	3,69	3.65	0.0166
	P (2 vs 4)	0.0135			
	P (3 vs 4)	-0.0160			

III. RESULTS

Tables I and II summarize the results of the LMM for all dependent variables. Table I reports the estimates for the effects of activation threshold and control signal conditions used during the first study and Table II reports the estimates for the effects of three speeds and four patterns used during the follow-up study. Fig. 5 depicts the average cross-correlation results for the three activation thresholds and two control signals used during the first study. Analysis of the cross-correlation of the expert–trainee movement showed significant main effects of the activation threshold ($p < 0.0001$) and control signal ($p < 0.0001$) conditions. However, the analysis did not show a significant interaction of the activation threshold $\times$ control signal conditions ($p = 0.1773$). A post-hoc analysis showed that the best cross-correlation values were achieved with the PD control signal regardless of the activation threshold and with the smallest activation threshold regardless of the control signal.

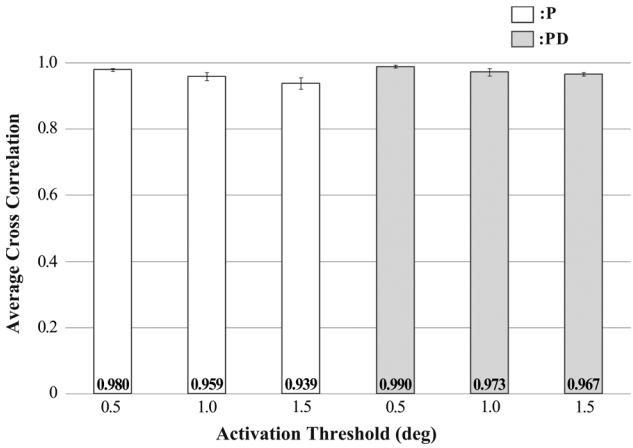

Fig. 5. Average expert–trainee cross-correlation results ($n = 5$) as a function of activation threshold and control signal. White and gray bars represent P and PD control signals, respectively. Error bars represent standard error of the mean.

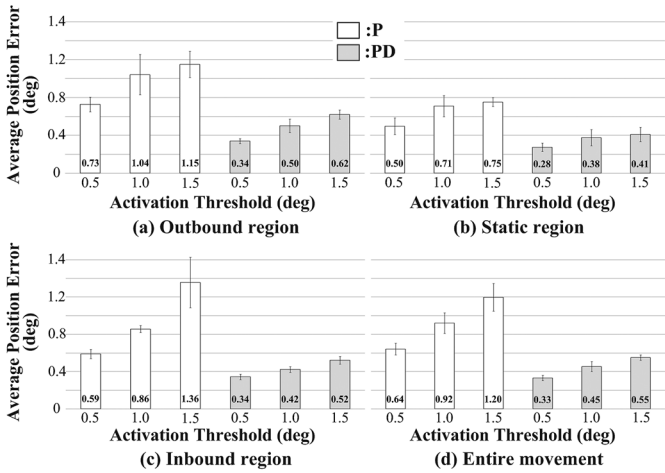

Fig. 6. Average expert–trainee position error results ($n = 5$) in degrees as a function of activation threshold and control signal by region. White and gray bars represent P and PD control signals, respectively. Error bars represent standard error of the mean.

Fig. 6 depicts the average expert–trainee position error for the outbound region (a), static region (b), inbound region (c), and entire movement (d). Analysis of the position error of the expert–trainee movement showed significant main effects of the activation threshold condition and control signal condition, respectively, for the outbound region ($p < 0.0001$ and $p < 0.0001$), static region ($p = 0.0016$ and $p < 0.0001$), inbound region ($p < 0.0001$ and $p < 0.0001$), and entire movement ($p < 0.0001$ and $p < 0.0001$). However, the analysis did not reveal a significant interaction of the activation threshold $\times$ control signal conditions for the outbound region ($p = 0.2416$), static region ($p = 0.8349$), or entire movement ($p = 0.3113$). Only the inbound region revealed a significant interaction of activation threshold $\times$ control signal conditions ($p = 0.0147$). A post-hoc analysis for the outbound and static regions and entire movement showed that subjects had smaller average position errors when using the PD control signal regardless of

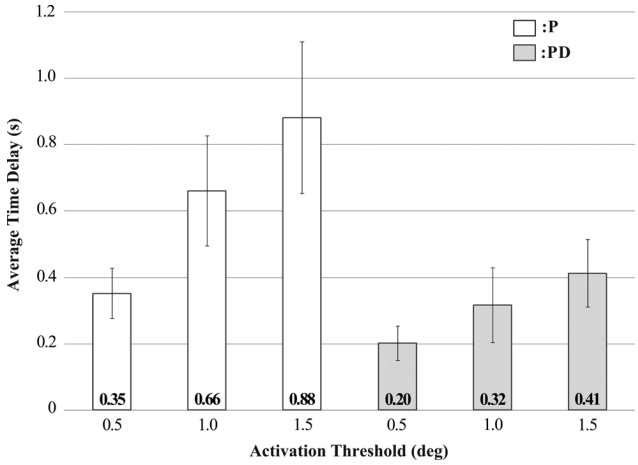

Fig. 7. Average expert–trainee time delay results $(n = 5)$ in seconds as a function of activation threshold limit and control signal. White and gray bars represent P and PD control signals, respectively. Error bars represent standard error of the mean.

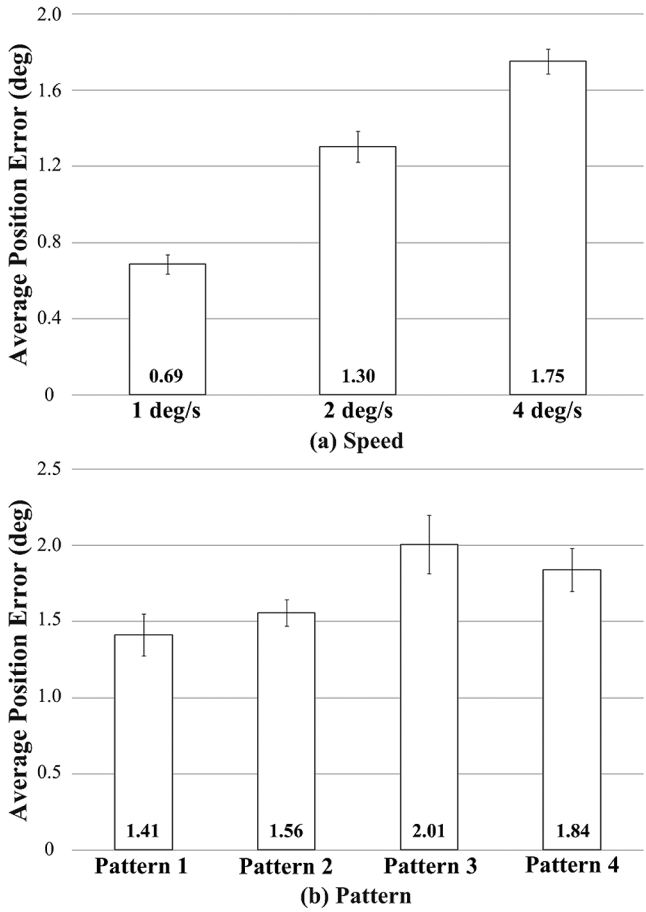

Fig. 8. Average expert–trainee position error results $(n = 8)$ in degrees as a function of (a) different speed conditions and (b) different pattern conditions. Error bars represent standard error of the mean.

the activation threshold and when using the smallest activation threshold regardless of the control signal. For the inbound region, however, a post-hoc analysis showed that the 0.5° activation threshold with the PD control signal resulted in the smallest average position error, but the three post-hoc pair-wise comparisons were not significant.

Fig. 7 represents the average time delay between the expert and subject movements over the entire movement. Analysis of the time delay of the expert–trainee movement showed significant main effects of activation threshold $(p < 0.0001)$ and control signal $(p = 0.0388)$ conditions, respectively. However, the analysis did not reveal a significant interaction of the activation threshold × control signal conditions $(p = 0.9941)$. A post-hoc analysis showed that subjects had the shortest time delays with the PD control signal regardless of activation threshold and with the smallest activation threshold regardless of control signal.

Fig. 8 depicts the average expert–trainee position error for the entire movement as a function of speed [Fig. 8(a)] and motion pattern [Fig. 8(b)]. Analysis of the motion replication data showed significant main effects on cross-correlation $(p < 0.0001)$ and position error $(p < 0.0001)$. Average cross-correlation values were found for slow (0.998), medium (0.992), and fast (0.985) speeds. A post-hoc analysis showed that subjects had the least amount of position error and the best cross-correlation value when they replicated the motion with the slowest speed. However, time delay was not significant $(p = 0.0535)$. Average time delays were found for slow (0.55 s), medium (0.63 s), and fast (0.52 s) speeds.

Analysis of the four motion patterns revealed significant main effects on cross-correlation $(p < 0.0001)$, position error $(p < 0.0001)$, and time delay $(p = 0.0166)$. Fig. 8(b) depicts the average expert–trainee position error for the entire movement by motion pattern. A post-hoc analysis showed that neither pattern 1 versus pattern 2 nor pattern 3 versus pattern 4 were significant in terms of position error. However, the subjects showed the least amount of position error when they performed either pattern 1 or 2 compared to pattern 3 and 4. In the case of cross-correlation performance, a post-hoc analysis showed the best cross-correlation value when the subjects performed pattern 1 versus patterns 2, 3, and 4. However, the pair-wise comparisons between patterns 2, 3, and 4 were not significant. The post-hoc analysis on time delay revealed that only the pair-wise comparison between patterns 1 and 2 was significant demonstrating that the subjects performed motion replication with the shortest time delay for pattern 1.

IV. Discussion

Based on the results of the first proof-of-concept study conducted in five healthy young adults, we demonstrated that subjects could accurately mimic the simple task of slowly bending at the waist using attractive vibrotactile instructional cues. The smallest error threshold (0.5°) combined with a proportional PD control signal resulted in the greatest correlation between the expert and trainee motion, the least amount of time delay, and the least amount of average position error. Subjects showed lower position errors during the static component of the entire movement than during the dynamic (inbound/outbound) components.

The PD control signal consistently produced significantly better motion replication in terms of cross-correlation, time delay, and average position error values compared to the P control signal for all error thresholds. This finding was not unexpected given that there is an inherent delay associated with

perceiving, processing, and responding to vibrotactile cues [18]. The inclusion of a rate of change of position term in the control signal effectively reduces the tactor activation threshold limit so that subjects receive information regarding their performance earlier than they would with a proportional-based control signal alone. Based on the average time delay results, the PD control signal decreased the lag in subject motion replication by 0.15 s, 0.34 s, and 0.47 s, for the 0.5°, 1.0°, and 1.5° error thresholds, respectively. In other words, as the error threshold increased, the PD control signal increasingly reduced the time lag compared to the P control signal. It may be possible to achieve equivalent performance using only a P control signal if the threshold limit were further reduced; however, if the limit is too small, motion will no longer be smooth. The choice of 0.5 ms as the constant weighting factor for the difference between expert and trainee velocity was chosen based on the study of Wall and Kentala [32]; it may be possible to further improve performance by manipulating this weighting factor since it was chosen arbitrarily in their study.

To date, vibrotactile feedback displays for standing balance [21], [37], [38] have used repulsive cues in which subjects are instructed to move away from the vibration. For the MIMIC, we chose to use attractive cues in which subjects were instructed to move toward the vibration. This decision was based on the results of an experiment that provided random nonmeaningful vibrotactile stimulation (i.e., no instructions provided regarding meaning of vibrotactile cues) to the trunk at the approximate level of the navel to naïve subjects. This study showed that tactors placed on top of the internal obliques and erector spinae resulted in small tilt deviations on the order of 1.0° in the direction of the tactor [39].

The results of the follow-up study in eight healthy young adults showed that the ability to accurately replicate motion decreased with increasing motion speed and complexity. Average position error increased as the required speed of the task increased. The slow speed from the first study was included as a control for the second study given that different subjects were involved. The average position error for the slow motion was smaller for the first study subjects compared to the second study subjects. This is likely due to the fact that the first group performed 18 practice trials compared to the three practice trials performed by the second group of subjects.

V. Conclusion

The results presented above indicate that subjects can successfully replicate prerecorded expert motions using the MIMIC, but that performance is dependent on the speed and complexity of the motion. The MIMIC platform has potential applications in both physical therapy settings and the athletic arena; it may be used to simultaneously instruct a classroom of trainees or by an individual at home to perform balance rehabilitation exercises either previously recorded in the presence of a physical therapist or distributed via the internet. Additionally, it may be used to gather data on the degree of replication and compliance to exercise schedule over months of training for analysis by a physical therapist. Although the MIMIC was designed to improve the ability of a trainee to mimic the motion of an expert using vibrotactile instructional cues, future versions of the technology might use stiffness or impedance control to enable the replication of forces and joint torques.

The main advantage of this design over that of either Lieberman [24] or Kapur [25] is that the IMUs eliminate the need for external apparati such as mechanical links, cameras, or magnetic emitters that are widely used in mechanical, optical, and electromagnetic tracking systems. From the device performance standpoint, this system supports accurate (better than 0.25°) and fast (100 Hz) motion estimation based on an EKF and component-based software architecture.

Acknowledgment

The authors would like to thank A. Galecki for guidance regarding the statistical analysis.

References

[1] F. B. Horak, C. Jones-Rycewicz, F. O. Black, and A. Shumway-Cook, "Effects of vestibular rehabilitation on dizziness and imbalance," *Otolaryngol. Head Neck Surg.*, vol. 106, no. 2, pp. 175–180, Feb. 1992.

[2] C. D. Mulrow, D. Gerety, J. E. Kanten, L. A. DeNino, L. Chiodo, M. B. Aguilar, C. O'Neil, J. Rosenberg, and R. M. Solis, "A randomized trial of physical rehabilitation for very frail nursing home residents," *J. Am. Med. Assoc.*, vol. 271, no. 7, pp. 519–524, Feb. 1994.

[3] C. Y. Crooks, J. M. Zumsteg, and K. R. Bell, "Traumatic brain injury: A review of practice management and recent advances," *Phys. Med. Rehabil. Clin. N. Am.*, vol. 18, no. 4, pp. 681–710, Nov. 2007.

[4] E. Y. Ones, K. Yalcinkaya, B. C. Toklu, and N. Caglar, "Effects of age, gender, and cognitive, functional and motor status on functional outcomes of stroke rehabilitation," *NeuroRehabilitation*, vol. 25, no. 4, pp. 241–249, Dec. 2009.

[5] P. M. Van Vliet and G. Wulf, "Extrinsic feedback for motor learning after stroke: What is the evidence?," *Disabil. Rehabil.*, vol. 28, no. 13–14, pp. 831–840, Jul. 2006.

[6] C. J. Winstein, "Knowledge of results and motor learning-implications for physical therapy," *J. Phy. Ther.*, vol. 71, no. 2, pp. 140–149, Feb. 1991.

[7] A. Domingo and D. P. Ferris, "Effects of physical guidance on short-term learning of walking on a narrow beam," *Gait Posture*, vol. 30, no. 4, pp. 464–468, Nov. 2009.

[8] D. E. Rumelhart, G. E. Hinton, and R. J. Williams, "Learning representations by back-propagating errors," *Nature*, vol. 323, no. 6088, pp. 533–536, Oct. 1986.

[9] S. G. Lisberger, "The neural basis for learning of simple motor skills," *Science*, vol. 242, no. 4879, pp. 728–735, Nov. 1988.

[10] M. A. Gutierrez, D. Thalmann, and F. Vexo, *Stepping Into Virtual Reality, a Practical Approach*, 2nd ed. Berlin, Germany: Springer, 2008.

[11] T. Debus, T. J. Jang, P. Dupont, and R. Howe, "Multi-channel vibrotactile display for teleoperated assembly," in *Proc. IEEE Int. Conf. Robot. Automat. (ICRA'02)*, Washington, DC, 2002, vol. 1, pp. 592–597.

[12] G. Moy, C. Wagner, and R. S. Fearing, "A compliant tactile display for teletaction," in *Proc. IEEE Int. Conf. Robot. Automat. (ICRA'00)*, San Francisco, CA, 2000, vol. 4, pp. 3409–3415.

[13] H. Kim, C. Seo, J. Lee, J. Ryu, S. Yu, and S. Lee, "Vibrotactile display for driving safety information," in *Proc. IEEE Intell. Transportat. Syst. Conf. (ITSC'06)*, Toronto, ON, Canada, 2006, pp. 573–577.

[14] Y. Yanagida, M. Kakita, R. W. Lindeman, Y. Kume, and N. Tetsutani, "Vibrotactile letter reading using a low-resolution tactor array," in *Proc. IEEE 12th Int. Symp. Haptic Interfaces Virtual Environment Teleoperator Syst. Haptics Symp.*, Chicago, IL, 2004, vol. 1, pp. 400–406.

[15] L. A. Jones, J. Kunkel, and E. Piateski, "Vibrotactile pattern recognition on the arm and back," *Perception*, vol. 38, no. 1, pp. 52–68, 2006.

[16] A. H. Rupert, B. J. McGrath, and M. Griffin, "A tool to maintain spatial orientation and situation awareness for operators of manned and unmanned aerial vehicles and other military motion platforms," in *RTO HFM Symp. Spatial Disorientat. Military Vehicles: Causes, Consequences Cures*, 2002, pp. 31.1–31.15.

[17] V. Chouvardas, A. Miliou, and M. Hatalis, "Tactile display applications: A state of the art survey," in *Proc. 2nd Balkan Conf. Informatics*, Ohrid, Macedonia, 2005, pp. 290–303.

[18] P. P. Kadkade, B. J. Benda, P. B. Schmidt, and C. Wall, "Vibrotactile display coding for a balance prosthesis," *IEEE Trans. Neural Syst. Rehabil. Eng*, vol. 11, no. 4, pp. 392–399, Dec. 2003.

[19] C. Wall and M. S. Weinberg, "Balance prostheses for postural control," *IEEE Eng. Med. Biol. Mag.*, vol. 22, no. 2, pp. 84–90, Mar. 2003.
[20] C. Wall, L. E. Oddsson, F. B. Horak, D. W. Wrisley, and M. Dozza, "Applications of vibrotactile display of body tilt for rehabilitation," in *Proc. IEEE 26th Ann. Int. Conf. Eng. Med. Biol. Soc. (EMBS'04)*, San Francisco, CA, 2004, pp. 4763–4765.
[21] K. H. Sienko, M. D. Balkwill, L. I. Oddsson, and C. Wall, "Effects of multi-directional vibrotactile feedback on vestibular-deficient postural performance during continuous multi-directional support surface perturbations," *J. Vestib. Res.*, vol. 18, no. 5–6, pp. 273–285, Jul. 2008.
[22] D. Ursu, L. T. Jiang, and K. H. Sienko, "Effect of vibrotactile trunk tilt feedback on postural stability in older adults," in *Proc. Ann. Am. Soc. Biomechan. Meeting*, 2009, pp. 26–29.
[23] P. Shull, K. Lurie, S. Mihye, T. Besier, and M. Cutkosky, "Haptic gait retraining for knee osteoarthritis treatment," in *Proc. IEEE Haptics Symp.*, Waltham, MA, 2010, pp. 409–416.
[24] J. Lieberman and C. Breazeal, "Development of a wearable vibrotactile feedback suit for accelerated human motor learning," in *Proc. IEEE Int. Conf. Robot. Automat. (ICRA'09)*, Kobe, Japan, 2007, pp. 4001–4006.
[25] P. Kapur, M. Jensen, L. J. Buxbaum, S. A. Jax, and K. J. Kuchenbecker, "Spatially distributed tactile feedback for kinesthetic motion guidance," in *Proc. IEEE Haptics Symp.*, Waltham, MA, 2010, pp. 519–526.
[26] F. Sergi, D. Accoto, D. Campolo, and E. Guglielmelli, "Forearm orientation guidance with a vibrotactile feedback bracelet: On the directionality of tactile motor communication," in *Proc. IEEE Int. Conf. Biomed. Robotics Biomechatron. (BIOROB'08)*, Washington, DC, 2008, pp. 433–438.
[27] J. van der Linden, E. Schoonderwaldt, and J. Bird, "Towards a real-time system for teaching novices correct violin bowing technique," in *Proc. IEEE Int. Workshop Haptic Audio Visual Environments Games (HAVE'09)*, Lecco, Italy, 2009, pp. 81–86.
[28] E. R. Bachmann, Y. Xiaoping, D. McKinney, R. B. McGhee, and M. J. Zyda, "Design and implementation of marg sensors for 3-DOF orientation measurement of rigid bodies," in *Proc. IEEE Int. Conf. Robot. Automat. (ICRA'03)*, Taipei, Taiwan, 2003, pp. 1171–1178.
[29] Z. Rong and Z. Zhaoying, "A real-time articulated human motion tracking using tri-axis inertial/magnetic sensors package," *IEEE Trans. Neural Syst. Rehabil. Eng.*, vol. 12, no. 2, pp. 295–302, Jun. 2004.
[30] A. M. Sabatini, C. Martelloni, S. Scapellato, and F. Cavallo, "Assessment of walking features from foot inertial sensing," *IEEE Trans. Biomed. Eng.*, vol. 52, no. 3, pp. 486–494, Mar. 2005.
[31] M. S. Weinberg, C. Wall, J. Robertsson, E. O'Neil, K. Sienko, and R. Fields, "Tilt determination in mems inertial vestibular prosthesis," *J. Biomech. Eng.*, vol. 128, no. 6, pp. 943–956, Dec. 2006.
[32] C. Wall and E. Kentala, "Effect of displacement, velocity, and combined vibrotactile tilt feedback on postural control of vestibulopathic subjects," *J. Vestib. Res.*, vol. 20, no. 1, pp. 61–69, Jan. 2010.
[33] D. E. Leader, "Kalman filter estimation of underwater vehicle position and attitude using a doppler velocity aided inertial motion unit" Ph.D. dissertation, Massachusetts Inst. Technol., Boston, MA, 1994.
[34] J. Vaganay, M. J. Aldon, and A. Fournier, "Mobile robot attitude estimation by fusion of inertial data," in *Proc. IEEE Int. Conf. Robot. Automat. (ICRA'93)*, Atlanta, GA, 1993, pp. 277–282.
[35] X. Yun and E. R. Bachmann, "Design, implementation, and experimental results of a quaternion-based kalman filter for human body motion tracking," *IEEE Trans. Robot.*, vol. 22, no. 6, pp. 1216–1227, Dec. 2006.
[36] A. D. Goodworth, C. Wall, and R. J. Peterka, "Influence of feedback parameters on performance of a vibrotactile balance prosthesis," *IEEE Trans. Neural Syst. Rehabil. Eng*, vol. 17, no. 4, pp. 397–408, Aug. 2006.
[37] E. Kentala, J. Vivas, and C. Wall, "Reduction of postural sway by use of a vibrotactile balance prosthesis prototype in subjects with vestibular deficits," *Ann. Otol. Rhinol. Laryngol.*, vol. 112, no. 5, pp. 404–409, May 2003.
[38] C. Wall and E. Kentala, "Control of sway using vibrotactile feedback of body tilt in patients with moderate and severe postural control deficits," *J. Vestib. Res*, vol. 15, no. 5–6, pp. 313–315, Apr. 2005.
[39] B. C. Lee, B. J. Martin, and K. H. Sienko, "Directional postural responses induced by vibrotactile stimulations applied to the torso".

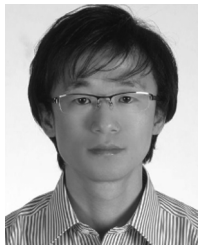

Beom-Chan Lee received the B.S. degree in electricity, electronics, information and telecommunication engineering from Kangwon National University (KNU), Korea, in 2004, and the M.S. degree in mechatronics from the Gwangju Institute of Science and Technology (GIST), Korea, in 2006. He is currently working toward the Ph.D. degree in the Department of Mechanical Engineering at University of Michigan, Ann Arbor.

He is currently with the Sensory Augmentation and Rehabilitation Laboratory, Department of Mechanical Engineering, University of Michigan, Ann Arbor.

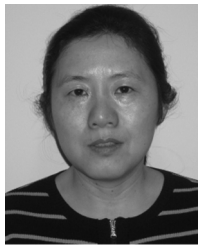

Shu Chen received the B.S. (1989) and M.S. (1992) degrees in chemical engineering from Hunan University, Hunan Province, China, and the M.S. degree in mathematics concentrated on computer science from Eastern Michigan University, Ypsilanti, in 2001.

She is currently working as a Senior Research Laboratory Specialist in the Institute of Gerontology, Department of Internal Medicine, at the University of Michigan, Ann Arbor.

Kathleen H. Sienko (M'07) received the B.S. degree in materials engineering from the University of Kentucky, Lexington, in 1998, S.M. degree in aeronautics and astronautics from the Massachusetts Institute of Technology (MIT), Cambridge, in 2000, and the Ph.D. degree in medical engineering and bioastronautics from the Harvard-MIT Division of Health Sciences and Technology, Cambridge, in 2007.

She was a Research Engineer with the Massachusetts Eye and Ear Infirmary, Harvard Medical School, Boston, MA. She is currently an Assistant Professor in the Departments of Mechanical and Biomedical Engineering at the University of Michigan, Ann Arbor, where she is also the Director of the Sensory Augmentation and Rehabilitation Laboratory.

Prof. Sienko is a member of American Society of Mechanical Engineers and American Society for Engineering Education.